REGENERATIVE MEDICINE

STEM CELLS

Allogeneic adipose-derived stem cells promote ischemic muscle repair by inducing M2 macrophage polarization via the HIF-1α/IL-10 pathway

Junchao Liu[1] | Peng Qiu[1] | Jinbao Qin[1] | Xiaoyu Wu[1] | Xin Wang[1] |
Xinrui Yang[1] | Bo Li[1] | Wenjie Zhang[2] | Kaichuang Ye[1] | Zhiyou Peng[1] |
Xinwu Lu[1,3]

[1]Department of Vascular Surgery, Shanghai Ninth People's Hospital, Shanghai JiaoTong University School of Medicine, Shanghai, People's Republic of China

[2]Shanghai Key Laboratory of Tissue Engineering, Shanghai Ninth People's Hospital, Shanghai JiaoTong University School of Medicine, Shanghai, People's Republic of China

[3]Vascular Center of Shanghai JiaoTong University, Shanghai, People's Republic of China

Correspondence
Xinwu Lu, MD, PhD, Zhiyou Peng, MD, PhD, and Kaichuang Ye, MD, PhD, Department of Vascular Surgery, Shanghai Ninth People's Hospital, Shanghai JiaoTong University School of Medicine, 639 Zhizaoju Road, Shanghai 200011, People's Republic of China.
Email: luxinwu@shsmu.edu.cn (X. L.), zhiyoupeng@163.com (Z. P.), and ykaichuang@163.com (K. Y.)

Abstract

Adipose-derived mesenchymal stem cells (ASCs) are multipotent stromal cells that possess considerable therapeutic potential for tissue remodeling. However, their protective mechanism in critical limb ischemia has not been fully defined. After the occlusion of blood vessels, hypoxia becomes a prominent feature of the ischemic limb. This study investigated the immunomodulatory effect of ASCs on ischemic muscle repair and explored the specific mechanism. We found that the ability of RAW264.7 cells to migrate was impaired in hypoxia, whereas coculturing with ASCs could enhance the migration capacity. In addition, under hypoxic conditions, the paracrine effect of ASCs was enhanced and ASCs could induce RAW264.7 macrophages toward the anti-inflammatory M2 phenotype. We further demonstrated that ASCs-derived interleukin 10 (IL-10), mediated by hypoxia inducible factor-1α (HIF-1α), played a crucial role in the induction of M2 macrophages by activating the signal transducer and activator of transcription 3 (STAT3)/Arginase (Arg-1) pathway. Our in vivo experiments revealed that transplanted ASCs exhibited an immunomodulatory effect by recruiting macrophages to ischemic muscle and increasing the density of M2 macrophages. The transplantation of ASCs into ischemic limbs induced increased blood flow reperfusion and limb salvage rate, whereas the depletion of tissue macrophages or transplanting HIF-1α-silenced ASCs inhibited the therapeutic effect. These findings elucidated the critical role of macrophages in ASCs-mediated ischemic muscle repair and proved that allogeneic ASCs could exert the protective effect by enhancing the recruitment of macrophages and inducing macrophages toward M2 phenotype through HIF-1α/IL-10 pathway.

KEYWORDS
adipose stem cells, angiogenesis, cell transplantation, hypoxia, skeletal muscle

---

Junchao Liu and Peng Qiu contributed equally to this study.

1 | INTRODUCTION

Critical limb ischemia (CLI) is the end stage of peripheral arterial disease, which is caused mainly by atherosclerosis. Although there are many intraluminal techniques for treating CLI, a high percentage of patients are not eligible for conventional revascularization, eventually leading to death or amputation.[1-3] The promotion of angiogenesis and collateral vessel establishment is thought to be the effective strategy for the treatment of CLI. As of recently, cell-based therapy is considered as a promising way to promote angiogenesis and tissue repair in CLI,[4] for which adipose-derived stem cells (ASCs) have been widely studied.

ASCs are isolated from adipose tissue and have the potential for multidirectional differentiation, such as osteoblasts, adipocytes, and endothelial cells. Owing to the character of sufficient source, easy isolation, and rapid proliferation, ASCs have been recognized as attractive candidates for cellular therapy in regenerative medicine.[5-7] Recently, issues have driven much interest in allogeneic stem cells for regeneration therapy, in which cells obtained from health donors can be quality-controlled and readily available as an "off-the-shelf" product for urgent application in clinical.[8,9] Previous studies by us[10-12] and others[13,14] have confirmed the significance of allogeneic ASCs in ischemic muscle repair, whereas the specific mechanism has seldom been explored. Recently, researchers have demonstrated that the function of mesenchymal stem cells (MSCs) in promoting tissue repair is mainly related to their paracrine effect rather than their direct implantation and differentiation.[15,16] Therefore, the illustration of the specific mechanism by which ASCs contribute to ischemic tissue repair is important for the translational application of ASCs in the future.

Inflammation has been shown to play an important role in tissue repair and angiogenesis.[17,18] Macrophages, recognized as the central cell of inflammatory response, have been extensively explored in recent years. During inflammation, circulating monocytes can be recruited to ischemic tissue and subsequently differentiate into macrophages. Studies have demonstrated that both monocyte-derived macrophages and tissue-resident macrophages are important for tissue repair and remodeling.[19,20] Macrophages are commonly classified into two distinct subsets: classically activated (M1) macrophages and alternatively activated (M2) macrophages. Different from M1 macrophages, M2 macrophages typically promote angiogenesis and tissue remodeling by releasing varieties of cytokines, chemokines, and other mediators.[21] Due to the occlusion of vessels or their inability to grow, hypoxia becomes a prominent feature of various diseases, including malignant tumors, ischemic limbs, and myocardial infarcts.[22-24] Previous studies have confirmed that MSCs exhibit better stemness and enhanced paracrine effect under hypoxic conditions.[25,26] In addition, MSCs have been shown to display anti-inflammatory and therapeutic effects on skin, arthrosis, and muscle by interacting with macrophages.[27-29] Therefore, considering the importance of M2 macrophages and hypoxic property in ischemic muscle, we hypothesized that hypoxia-activated ASCs could exert the therapeutic effect on ischemic muscle by selectively inducing macrophages toward M2 phenotype.

In this study, we explored the effects of ASCs on macrophages under hypoxic conditions and whether the interaction plays a vital role in ischemic muscle repair. Our results showed that ASCs could enhance the

Significance statement

This study focused on exploring the mechanism of allogeneic adipose-derived stem cells (ASCs) in critical limb ischemia repair. This study has also demonstrated that macrophages are critical in ASCs-mediated ischemic muscle repair and that transplanted ASCs can contribute to tissue remodeling by recruiting macrophages and inducing macrophages toward M2 phenotype. Mechanically, ASCs-derived interleukin 10 (IL-10), mediated by hypoxia inducible factor-1a (HIF-1a), plays the crucial role during the polarization process. The results obtained from this study could contribute to the translational application of allogeneic ASCs in ischemic limb repair and help to understand the interaction between stem cells and macrophages under ischemic conditions.

migration of RAW264.7 macrophages and induce them toward M2 phenotype in hypoxia. Besides, the osteogenic and adipogenic differentiation of ASCs were attenuated and the paracrine effect of ASCs was enhanced under hypoxic conditions. We also demonstrated the critical role of hypoxia inducible factor-1α (HIF-1α) in interleukin 10 (IL-10) production in ASCs and delineated the mechanism of M2 macrophages polarization induced by ASCs-derived IL-10 via the signal transducer and activator of transcription 3 (STAT3)/Arginase (Arg-1) pathway. In vivo results showed the increased density of vessels and M2 macrophages after the transplantation of ASCs into ischemic muscle, whereas the depletion of macrophages or transplanting HIF-1α-silenced ASCs reduced the therapeutic effect. These findings demonstrated that transplanted ASCs could contribute to ischemic muscle repair by increasing the recruitment of macrophages and inducing M2 macrophages polarization, with the HIF-1α/IL-10 pathway playing the critical role.

2 | MATERIALS AND METHODS

2.1 | Animals

All animal procedures were in accordance with the protocols approved by Animal Care and Use Committee of Shanghai Ninth People's Hospital, Shanghai Jiao Tong University, School of Medicine. 8 to 9-week old C57BL/6 wild-type male mice were purchased from the Shanghai Research Center for Model Organisms (Shanghai, China) and housed in the animal vivarium of Shanghai Ninth People's Hospital Central Laboratory.

2.2 | Isolation, culture, and characterization of ASCs

ASCs were isolated from the subcutaneous adipose tissues of the inguinal area of C57BL/6 wild-type female mice. The obtained

adipose tissues were incubated with NB4 collagenase solution (Nordmark, Uetersen, German) in Dulbecco's modified Eagle's medium (DMEM), which was supplemented with 10% fetal bovine serum (Gibco, Waltham, Massachusetts) and 1% streptomycin/penicillin (Sigma, St. Louis, Missouri). After 60 minutes shaking (250 rpm) at 37°C, the cells were centrifuged and placed on culture dishes. Passage 3 ASCs were collected and used for the following experiments.

2.3 | Alizarin red staining and red oil staining

To examine the adipogenic and osteogenic differentiation capacity of the isolated cells, the mouse Mesenchymal Stem Cell Functional Identification Kit (Cyagen, SuZhou, China) was used to assess the differentiation of ASCs under normoxic and hypoxic conditions. ASCs (10^5 cells/well) were plated in six-well plates and cultured in a 5% CO_2 humidified incubator. The supernatant was replaced with adipogenic and osteogenic differentiation medium after ASCs reaching 70% to 80% confluence. Then plates were placed in normoxic incubator (20% O_2) or hypoxic incubator (1% O_2), respectively, and the supernatant was refreshed every 2 to 3 days. Alizarin Red staining and Red Oil staining were conducted on day 21 to evaluate the ability of the ASCs to differentiate into osteoblasts and adipocyte. Cells were photographed using a fluorescence microscope (Olympus, Tokyo, Japan).

2.4 | Enzyme-linked immunosorbent assay

ASCs (10^5 cells/well) were seeded in six-well plates until reaching 70% to 80% confluence. Then the medium was replaced with serum-free DMEM and ASCs were cultured in normoxic (20% O_2) or hypoxic (1% O_2) incubator separately for 24 hours. The supernatant was collected and spun down to remove cells and debris. Enzyme-linked immunosorbent assay (ELISA) (MultiSciences, Shanghai, China) kit was used to measure the level of hepatocyte growth factor (HGF), transforming growth factor-β (TGF-β), basic fibroblast growth factor (b-FGF), vascular endothelial growth factor (VEGF), IL-10, IL-1β, tumor necrosis factor-α (TNF-α), and IL-6 to assess the secretory profile of ASCs in normoxic and hypoxic conditions. In addition, after finishing blood flow assessment on day 7, mice (three per group) were sacrificed and the gastrocnemius muscles were obtained and stored at −80°C until needed. To examine the level of IL-10 in muscles, the frozen muscles were homogenized and mixed with cell lysis buffer including proteases cocktail. After centrifuged at 4°C for 8 minutes at 5000 rpm, the supernatants were collected and the total protein concentration was measured using BCA Protein Assay Kit (Beyotime, Shanghai, China). Then supernatants were adjusted to the same protein concentration and the levels of IL-10 in the adjusted supernatants were detected using ELISA kit (MultiSciences, Shanghai, China) according to the manufacturer's instruction.

2.5 | Cell counting kit-8, EdU, and transwell assay

The mouse macrophage cell line, RAW264.7 cells, was obtained from the Shanghai Cell Bank, the Chinese Academy of Sciences (Shanghai, China). RAW264.7 cells (10^5 cells/well) were placed on the lower compartment of 24-well transwell plates (0.4 μm; Corning, New York) and three groups (RAW264.7^{Normo}, RAW264.7^{Hypo}, RAW264.7^{Hypo} + ASCs) were divided based on whether cultivated in hypoxia (1% O_2) and cocultured with ASCs (2×10^4 cells/well) in the upper chambers. After 24 hours cultivation, the upper chambers were removed and CCK-8 reagent (Dojindo Laboratories, Shanghai, China) was added to the lower compartment. Then the transwell plates were placed in cell incubator for 1 hour. Afterward, the supernatant was transferred into a 96-well plate to detect absorbance at 450 nm using microplate reader (Biotek, Winooski, Vermont). EdU proliferation assay was conducted with the use of Ethynyl-deoxyuridine assay (RiboBio, Guangzhou, China) according to the manufacturer instructions. For cell migration assay, Matrigel (Corning, New York) was applied to the upper chambers of 24-well transwell plates (8 μm; Corning, New York) and plates were placed into a 37°C incubator to polymerize Matrigel into gel. Then RAW264.7 cells (10^5 cells/well) were plated in the upper chambers and cultivated in hypoxic (1% O_2) incubator with ASCs (2×10^4 cells/well) seeded on the lower compartment of transwell plates. Twenty-four hours later, chambers were taken out and crystal violet staining was performed to evaluate the migration capacity of RAW264.7 cells.

2.6 | Small interfering RNA transfection

For *HIF-1α* gene silencing, small interfering RNA (SiRNA) transfection was performed using SiRNA from GenePharma. ASCs (10^5 cells/well) were plated on six-well plates until reaching 70% to 80% confluence. Then cells were washed with phosphate buffer saline (PBS) and transfected with *HIF-1α*-SiRNA, or nontargeting SiRNA (Scrambled SiRNA) using lipofectamine 3000 (Thermo Fisher Scientific, Waltham, Massachusetts) according to the manufacturer's protocol. After 6 to 8 hours incubation, the transfection medium was replaced with fresh DMEM and plates were transferred into the hypoxic (1% O_2) incubator. After additional 48 hours cultivation, real-time quantitative PCR (RT-qPCR) and Western blot were performed using *HIF-1α*-specific primers and HIF-1α primary antibody (CST-36169), respectively, to evaluate the knockdown efficiency. In addition, the morphology and proliferation capacity of ASCs with and without SiRNA transfection were also detected.

2.7 | Detection of macrophages polarization

To detect the effect of ASCs on macrophages polarization, RAW264.7 cells (5×10^5 cells/well) were cultivated in six-well transwell plates for 24 hours under hypoxic (1% O_2) conditions with ASCs (10^5 cells/well) coculturing. Anti-IL-10 (0.1 μg/mL; BD Bioscience, Franklin Lakes, New Jersey), a neutralizing antibody to IL-10, was added to the

coculturing system to examine the function of IL-10 in the polarization process. Flow cytometric analysis was performed to confirm cells phenotype after 24 hours cultivation. To further analyze the polarization effect, RT-qPCR was performed to detect the expression of polarization-related genes, including *Arg-1*, *Mrc-1*, *IL-10*, *IL-1β*, *TNF-α*, and *IL-6*. The specific primers sequences used for RT-qPCR are listed in Table S1. To reveal the mechanism of ASCs on the polarization of RAW264.7 macrophages in hypoxia, the conditioned medium of ASCs cultivated in hypoxic conditions (CM-ASCs) was collected to incubate RAW264.7 macrophages. STAT3 inhibitor S3I-201 (400 μM; Absin, Shanghai, China) and Anti-IL-10 (0.1 μg/mL) were applied to the culturing system. RAW264.7 macrophages (5×10^5 cells/well) were cultivated in hypoxia (1% O_2) and divided into four groups according to different treatments: (a) Control, (b) CM-ASCs, (c) CM-ASCs+Anti-IL-10 (same as [b] but with Anti-IL-10), and (d) CM-ASCs+S3I-201 (same as [b] but with S3I-201). After 24 hours cultivation, RAW264.7 macrophages were obtained and Western blot was used to measure the expression polarization-related proteins: Arg-1 (CST-93668), STAT3 (CST-12640), and P-STAT3 (CST-9145).

2.8 | Flow cytometry analysis

To identify the characteristic of ASCs and RAW264.7 cells, the expression of surface antigens (CD29, CD90, CD44, CD34, CD31, CD68, F4/80, CD206) was analyzed by incubating ASCs or RAW264.7 cells with the respective antibodies in 100 μL FACS buffer (Sigma, San Francisco, California). The following antibodies were used for analysis: fluorescein isothiocyanate (FITC)-conjugated mouse antibodies against CD29 (Biolegend-102 205), CD90 (Biolegend-105 305), CD44 (Biolegend-103 021), CD31 (Biolegend-102 405), CD34 (eBioscience-11-0341-82), and PE-conjugated mouse antibodies against CD68 (Biolegend-137 013), F4/80 (Biolegend-123 110), allophycocyanin (APC)-conjugated mouse antibody against CD206 (Biolegend-141 708). The unstained samples were used to detect autofluorescence and set the photomultiplier for the used channels. Stained cells were washed twice in 1.5 mL FACS buffer and fixed with Cytofix (BD Pharminogen, San Diego, California). Samples were analyzed using the ACEA NovoCyte flow cytometer and the collected data were processed with FlowJo software.

2.9 | Local transplantation and macrophage depletion

C57BL/6 mice (8- to 9-week, male, n = 40) were used for the establishment of hind limb ischemia model. The right femoral artery and its branches were ligated as described previously.[30] After being anesthetized with 3% pentobarbital sodium, the mouse was fixed on board and femoral artery was exposed from the inguinal ligament to the bifurcation of the popliteal artery. Then 9-0 silk suture was used to ligate the proximal origin of femoral artery and popliteal artery, and the artery between the two ligatures was excised. ASCs, ASCs[Si-HIF-1α],

or PBS were intramuscularly injected into the ischemic hind limbs and the mice were divided into four groups: ASCs, ASCs[Si-HIF-1α], ASCs + Mφ[clear], and PBS, respectively (10^6 cells in 100 μL PBS per mouse). In ASCs + Mφ[clear] group, tissue macrophages were depleted using clodronate liposomes solution (0.2 mL/25 g, Target Technology, Beijing, China) through intravenous injection using 26-gauge needle.

2.10 | Blood flow evaluation and histological analysis

The hind limb blood flow was measured using laser Doppler perfusion imaging analyzer (Moor Instruments, Devon, UK) on days 0, 7, and 21. The gastrocnemius muscles obtained on day 7 were embedded in paraffin and used for histochemical analysis. The tissues were sectioned into 6 to 8 μm slices and incubated with rabbit monoclonal antibody (mAb) directed against CD68 (Abcam-ab125212) and CD206 (Abcam-ab64693) to locate M2 macrophages. Besides, Arginase-1 (Arg-1) were also stained by incubating with Rabbit mAb against Arg-1 (Abcam-ab91279) to detect the expression of Arg-1 in vivo. Moreover, the ischemic muscle of mice (seven per group) was obtained on day 21 and sectioned into slices as disposed above. Then, tissue slices were incubated with Rabbit mAb against CD31 (Abcam-ab28364) to identity vascular density. In addition, H&E staining was also performed to evaluate the degree of muscle degeneration and necrosis. The stained sections were imaged under Olympus fluorescence microscopy. The average count of three fields was calculated and each specimen was analyzed with three slices.

2.11 | Statistical analysis

Quantitative data were described as means ± SD of at least three independent experiments. Unpaired two-tailed Student's *t* test was used to compare means between groups and the differences among multiple groups were analyzed with one-way analysis of variance. The *P* value below .05 was defined as statistically significant. The comparison results were labeled with * for *P* value < .05, ** for *P* value < .01 and *** for *P* value < .001. All statistical analyses were conducted using GraphPad Prism Version 6.0a (GraphPad Software, La Jolla, California).

3 | RESULTS

3.1 | Characterization of ASCs and RAW264.7 cells

After isolating ASCs from C57B/L mice, we adopted the passage 3 (Figure 1A) cells for our experiment. Flow cytometry analysis showed that the ASCs were strongly positive for MSC surface antigens (CD29, CD90, and CD44), whereas almost no hematopoietic cell makers (CD34 and CD31) were detected (Figure 1B). In addition, flow cytometry and cellular immunofluorescence experiments were used
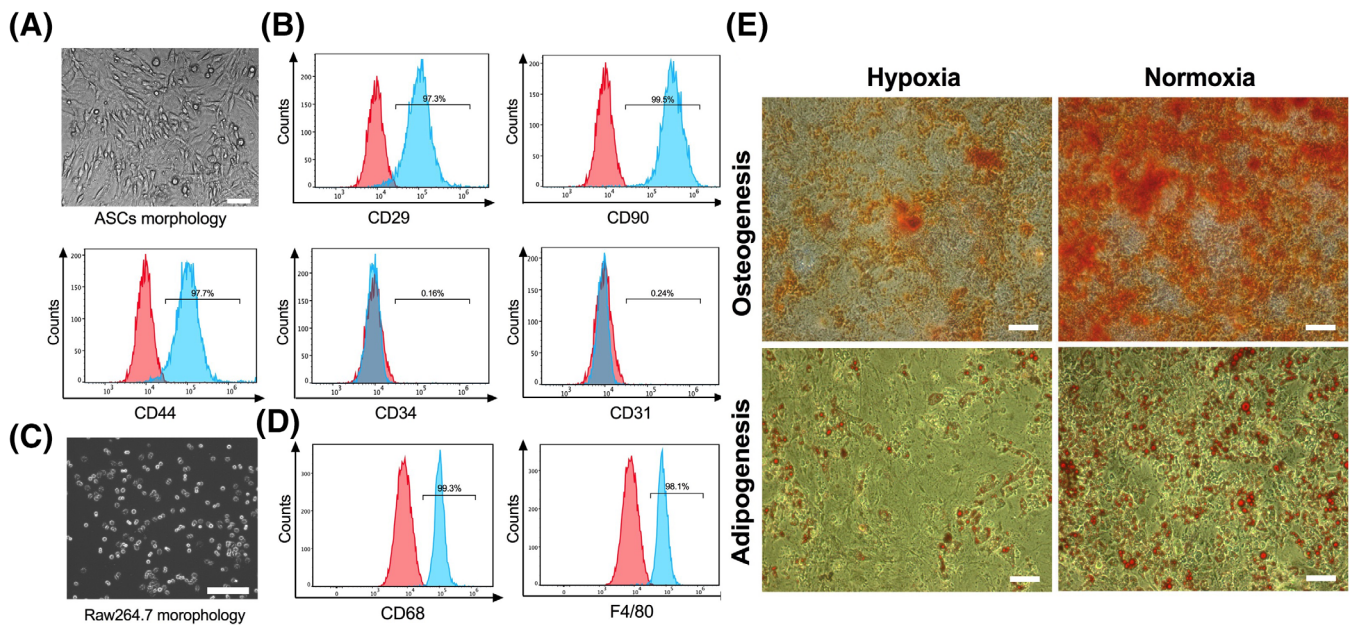
FIGURE 1 The characterization of ASCs and RAW264.7 cells and the detection of ASCs differentiation. A, Representative image of ASCs in passage 3. B, Flow cytometry histograms of ASCs exhibiting strongly positive expression of CD29, CD90, and CD44 as well as negative expression of CD31 and CD34. C, Representative image of RAW264.7 cells. D, Flow cytometry histograms of RAW264.7 cells showing remarkably positive for CD68 and F4/80. E, Representative images of the osteogenesis and adipogenesis of ASCs under normoxic or hypoxic conditions. Scale bar = 200 μm. ASCs, adipose-derived mesenchymal stem cells

for phenotypic analysis of the RAW264.7 cells (Figure 1C), which was shown to be remarkably positive for the macrophage-specific surface markers CD68 and F4/80 (Figures 1D and S1).

3.2 | Osteogenesis and adipogenesis differentiation of ASCs under normoxic and hypoxic conditions

After cultivated in 1% O_2 or 20% O_2 cell incubator for 21 days, ASCs were stained separately with Alizarin Red and Red Oil reagent. Results showed that osteogenesis differentiation in hypoxic group was significantly less than that of normoxic group. Similarly, fewer ASCs in hypoxic group differentiated into adipocytes compared with normoxic group (Figures 1E and S2A,B). These results demonstrated that hypoxia inhibited the osteogenesis and adipogenesis differentiation of ASCs, implying the reduced repair potential of ASCs through direct differentiation after transplanted into ischemic muscles.
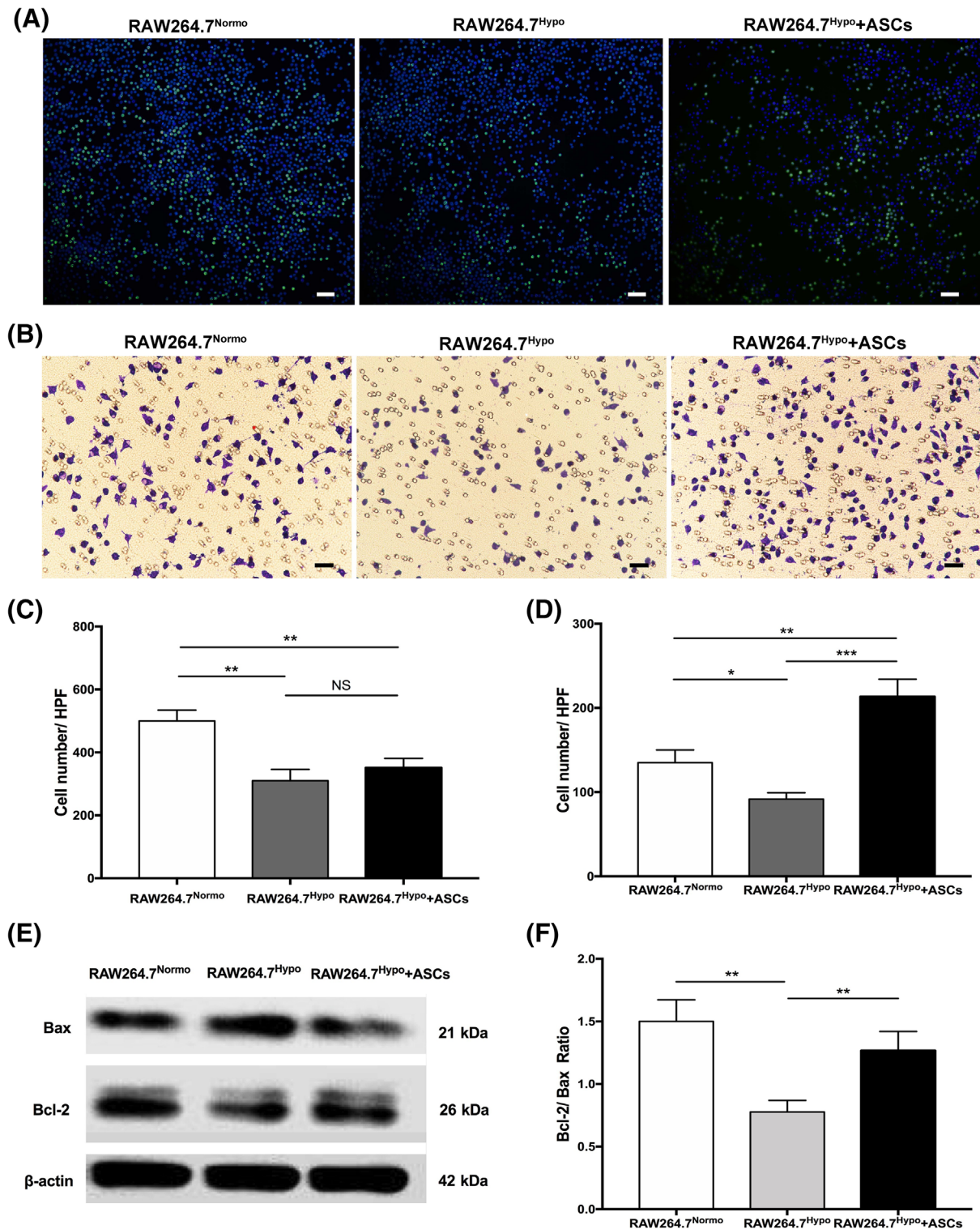
3.3 | Effect of ASCs on the proliferation, migration, and viability of macrophages

To clarify the effect of ASCs on macrophages in hypoxia, RAW264.7 cells were cocultured with ASCs under hypoxic conditions. Then the proliferation, migration, and viability of RAW264.7 cells were evaluated separately. 5-Ethynyl-29-deoxyuridine (EdU) incorporation assay showed that hypoxia reduced the number of EdU$^+$ cells and that ASCs

did not drive significantly more RAW264.7 cells into the EdU$^+$ S phase (Figure 2A,C). In addition, the CCK-8 assay showed that hypoxia inhibited the proliferation of RAW264.7 cells and that coculturing with ASCs had no impact on the proliferation capacity (Figure S3). The ability to migrate is a critical feature of macrophages that allows them to appear in damaged tissues and exert anti-inflammatory and tissue-repairing effects in a timely manner. A transwell migration assay was conducted to test the migratory ability of RAW264.7 cells in our work. Significantly fewer cells in RAW264.7^{Hypo} group were observed on the bottom membrane of transwell chamber, whereas the number of cells increased significantly after coculturing with ASCs (Figure 2B,D). These results indicate that hypoxia may impair the ability of macrophages to migrate, whereas ASCs could enhance the recruitment of macrophages in hypoxia. Besides, we also investigated the viability of RAW264.7 cells through Western blot assay (Figure 2E,F). Compared with normoxic group, RAW264.7 cells cultivated in hypoxia had a higher expression of the Bax protein and a lower expression of the Bcl-2 protein. However, the effect was reversed after coculturing with ASCs, indicating that ASCs may help to prevent the apoptosis of macrophages caused by hypoxia.

3.4 | Detection of ASC paracrine factors under normoxic and hypoxic conditions

The paracrine factors of MSCs play an important role in tissue repair. To investigate the paracrine effect of ASCs under hypoxic conditions, the supernatant media of ASCs cultured in 20% O_2 and 1% O_2 were

FIGURE 2 The effect of ASCs on the proliferation, migration, and viability of RAW264.7 cells. A, Representative images of macrophages EdU proliferation assay in RAW264.7^{Normo}, RAW264.7^{Hypo}, RAW264.7^{Hypo} + ASCs groups. B, Representative images of transwell assay in RAW264.7^{Normo}, RAW264.7^{Hypo}, RAW264.7^{Hypo} + ASCs groups. C, Quantification chart of the average number of RAW264.7 cells in EdU^{+} S phage per HPF. D, Quantification chart of the number of migrated RAW264.7 cells on the bottom membrane per HPF. E, Representative Western blot image to evaluate the expression of apoptosis-related proteins in RAW264.7 cells. F, Quantification chart of the relative ratio of Bcl-2 and Bax. At least three independent experiments were performed with each experiment. *P < .05; **P < .01; ***P < .001. Scale bar = 100 μm. ASCs, adipose-derived mesenchymal stem cells; HPF, high power field; NS, not significant; RAW264.7^{Hypo} + ASCs, RAW264.7 cells co-cultivated with ASCs in hypoxic condition; RAW264.7^{Hypo}, RAW264.7 cells cultivated in hypoxic condition; RAW264.7^{Normo}, RAW264.7 cells cultivated in normoxic condition

analyzed separately. ELISAs were used to measure the levels of HGF, TGF-β, b-FGF, VEGF, IL-1β, IL-10, TNF-α, and IL-6. Results showed that all measured cytokines, except TNF-α, significantly increased under hypoxic conditions, confirming the enhanced paracrine function of ASCs in hypoxia (Figure 3A).

3.5 | Effect and mechanism of ASCs on macrophage polarization under hypoxic conditions

Next, we analyzed the effect of ASCs on the polarization of macrophages and explored the specific mechanisms. Because of the significance of IL-10 in the polarization of macrophages, we analyzed the

mechanism of increased IL-10 secretion from ASCs in hypoxia and examined whether ASCs-derived IL-10 played a critical role in macrophage polarization. HIF-1α, a transcription factor enhanced by hypoxia, has been reported to participate in the regulation of a spectrum of genes that maintain homeostasis.[31] To assess whether HIF-1α mediates the expression of IL-10, we first explored the expression of HIF-1α in ASCs under normoxic and hypoxic conditions. The protein and gene expression of HIF-1α increased significantly in hypoxia (1% O_2) and decreased significantly after ASCs were transfected with SiRNA against HIF-1α (Figure 3B-D). The level of IL-10 secreted by ASCs and the gene expression of IL-10 within ASCs decreased significantly after silencing HIF-1α in ASCs (Figure 3E,F). Moreover, no significant difference about the morphology and proliferative ability of
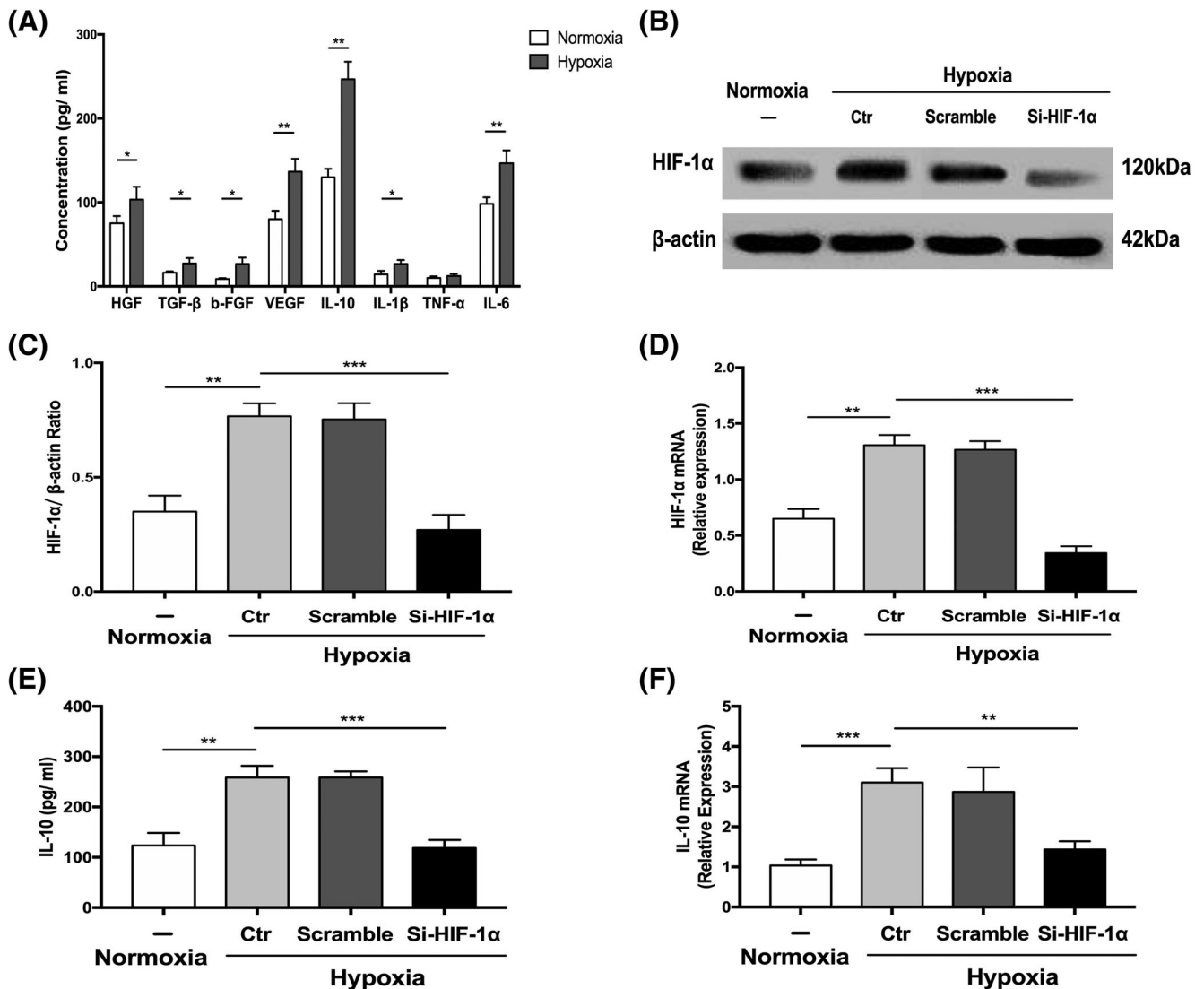
FIGURE 3   The enhanced paracrine effect and activated HIF-1α/IL-10 pathway in ASCs under hypoxic conditions. A, The paracrine effect of ASCs under normoxic and hypoxic conditions. B-D, Representative Western blot image (B) and quantification chart of the protein expression (C) and gene expression (D) to detect the knockdown efficiency of *HIF-1α*-SiRNA in ASCs. E,F, Quantification chart of the secretion of IL-10 from ASCs (E) and the gene expression of IL-10 in ASCs (F) after silencing *HIF-1α*. At least three independent experiments were performed with each experiment. *$P < .05$; **$P < .01$; ***$P < .001$. ASCs, adipose-derived mesenchymal stem cells; b-FGF, basic fibroblast growth factor; HGF, hepatocyte growth factor; IL-10, Interleukin-10; IL-1β, Interleukin-1β; IL-6, Interleukin-6; NS, not significant; Si-HIF-1α, HIF-1α specific small interfering RNA; TGF, tumor necrosis factor; TNF-α, tumor necrosis factor-α; VEGF, vascular endothelial growth factor

ASCs was found between groups with and without SiRNA transfection (Figure S4A,B). Our results demonstrated that HIF-1α mediated the increased expression of IL-10 in ASCs under hypoxic conditions.

To verify the effect of ASCs on macrophages polarization, flow cytometry was used to detect the percentage of CD206+ RAW264.7 macrophages. Significant higher percentage of CD206+ RAW264.7 macrophages was found after cultured with ASCs under hypoxic conditions, whereas the ratio decreased significantly with the addition of anti-IL-10 into the coculturing system (Figures 4A and S5). To further analyze cells phenotypes in different groups, we explored the expression of M1- and M2-related genes. The mRNA levels of *Arg-1*, *Mrc-1*, and *IL-10* increased significantly and the expression of the genes for *IL-1β*, *IL-6*, and *TNF-α* decreased after the coculture of RAW264.7 macrophages with ASCs in hypoxia, whereas anti-IL-10 significantly reduced the effect caused by cocultivation with ASCs (Figure 4B). These results confirmed the role of ASCs in driving macrophage polarization toward M2 phenotype and that IL-10 secreted by ASCs dominated the process. Previous studies have demonstrated that STAT3 binds to the promoter region of Arg-1 and increases the expression and activity of Arg-1.[32] To delineate the mechanism of ASCs-derived IL-10 in inducing M2 macrophages and detect the role of STAT3 in the process, RAW264.7 macrophages were incubated by CM-ASCs with anti-IL-10 or S3I-201. Results exhibited that the protein expression of Arg-1 and p-STAT3 was significantly upregulated in RAW264.7 macrophages after cultivated with CM-ASCs. However, the addition of anti-IL-10 or S3I-201 significantly reduced the protein expression of p-STAT3 and Arg-1 caused by CM-ASCs, demonstrating that ASCs-derived IL-10 dominated the increased expression of Arg-1 in RAW264.7 macrophages through STAT3 pathway (Figure 4C-E). Taken together, these results indicate that ASCs can induce RAW264.7 macrophages toward the M2 phenotype in hypoxia, during which ASCs-derived IL-10 plays a critical role via the STAT3/Arg-1 signaling pathway.

3.6 | Depletion of tissue macrophages or silencing HIF-1α in ASCs reduces the therapeutic effect of ASCs in hind limb ischemia

To further verify the underlying mechanism of tissue repair by ASCs, we established hind limb ischemia mice model and divided them into four groups (PBS, ASCs, ASCs + Mφ^{clear}, and ASCs$^{Si-HIF-1α}$).
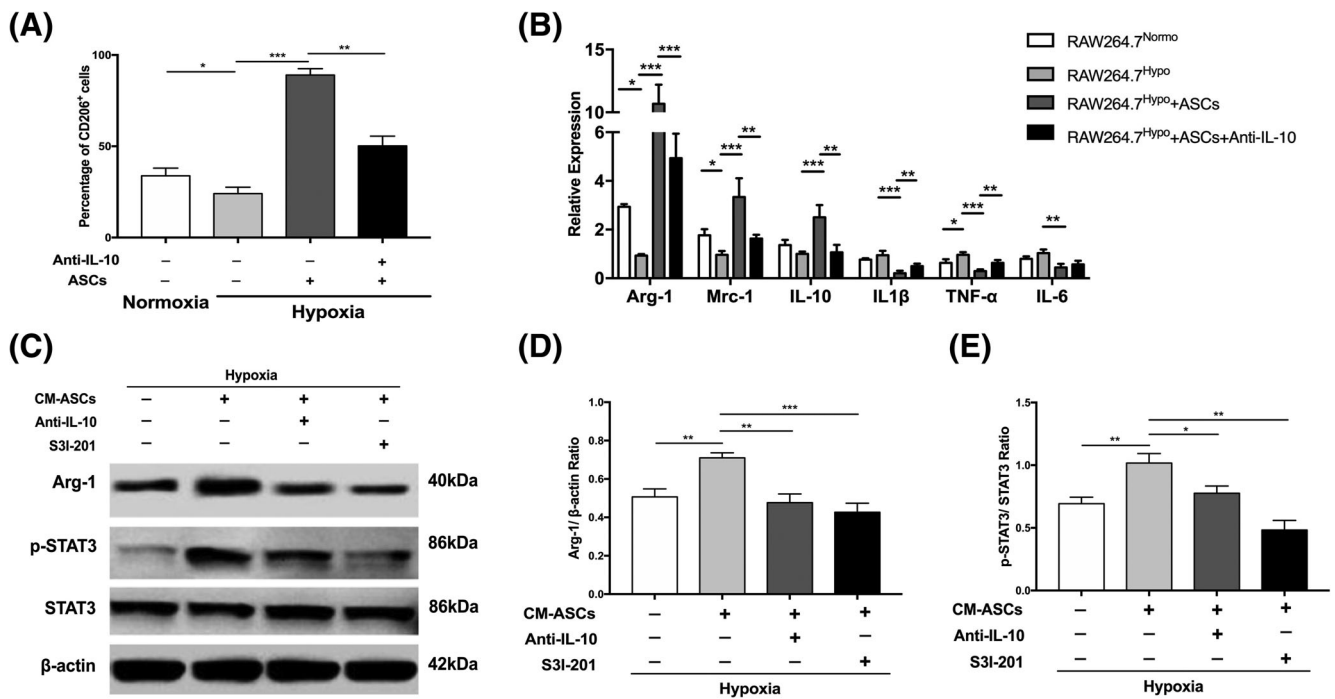

FIGURE 4 The effect and mechanism of ASCs on the polarization of RAW264.7 macrophages in hypoxia. A, The frequencies of CD206+ cells in RAW264.7^{Normo}, RAW264.7^{Hypo}, RAW264.7^{Hypo} + ASCs, and RAW264.7^{Hypo} + ASCs + Anti-IL-10 groups. B, The relative gene expression of M1-related genes (IL-1β, TNF-α, and IL-6) and M2-related genes (Arg-1, Mrc-1, and IL-10) in RAW264.7^{Normo}, RAW264.7^{Hypo}, RAW264.7^{Hypo} + ASCs, and RAW264.7^{Hypo} + ASCs + Anti-IL-10 groups. C-E, Western blot result to measure the protein expression of Arg-1, p-STAT3, and STAT3 in Control (RAW264.7 macrophages cultivated in hypoxia), CM-ASCs (RAW264.7 macrophages cultivated with CM-ASCs in hypoxia), CM-ASCs + Anti-IL-10 (RAW264.7 macrophages cultivated with CM-ASCs and Anti-IL-10 in hypoxia), and CM-ASCs + S3I-201 (RAW264.7 macrophages cultivated with CM-ASCs and S3I-201 in hypoxia) groups. β-actin was used as the internal control. At least three independent experiments were performed with each experiment. *P < .05; **P < .01; ***P < .001. Anti-IL-10, IL-10-neutralizing antibody; Arg-1, Arginase-1; ASCs, adipose-derived mesenchymal stem cells; CM-ASCs, conditioned medium of ASCs cultivated in hypoxia; IL-10, Interleukin-10; IL-1β, Interleukin-1β; IL-6, Interleukin-6; Mrc-1, mannose receptor-1; RAW264.7^{Hypo} + ASCs + Anti-IL-10, RAW264.7 macrophages cultivated with ASCs in hypoxia with the addition of Anti-IL-10; RAW264.7^{Hypo} + ASCs, RAW264.7 macrophages cultivated with ASCs in hypoxia; RAW264.7^{Hypo}, RAW264.7 macrophages cultivated in hypoxia; RAW264.7^{Normo}, RAW264.7 macrophages cultivated in normoxia; S3I-201, the STAT3 inhibitor; TNF-α, tumor necrosis factor-α

A schematic of the experimental design is shown in Figure 5A. Blood flow was measured using laser Doppler perfusion imaging (LDPI) on days 0, 7, and 21 and representative images of different groups were displayed in Figure 5B. Quantitative analysis revealed that blood reperfusion recovered much better in the ASCs group than in the ASCs + Mφ^{clear} group and the PBS group, indicating that macrophages play a critical role in tissue angiogenesis. In addition, blood reperfusion in the ASCs$^{Si-HIF-1\alpha}$ group was significantly worse than that in the ASCs group (Figure 5B,C), implying that HIF-1α plays a critical role in ASCs-mediated tissue repair. The prognosis of the ischemic hind limbs was evaluated on day 21. Consistent with the blood flow results, the number of hind limbs with necrosis or amputation in the ASCs group was less than that in the other three groups, and nearly all hind limbs in the ASCs + Mφ^{clear} group suffered necrosis or amputation, which was comparable to the case of the PBS group (Figure 5D).

3.7 | Histological analysis of the ischemic hind limb muscle

On day 7, ischemic hind limbs were obtained for histological analysis. To evaluate the density of macrophages (CD68$^+$) and M2 macrophages (CD68$^+$/CD206$^+$) in ischemic muscle, tissue sections were costained for CD68 and CD206. The number of macrophages in the ASCs group was significantly higher than that of ASCs + Mφ^{clear} and PBS groups but similar to that of ASCs$^{Si-HIF-1\alpha}$ group (Figure 6A,B). Furthermore, the density of M2 macrophages in the ASCs group was significantly higher than that of other three groups, including the ASCs$^{Si-HIF-1\alpha}$ group (Figure 6A,C). Immunofluorescence analysis also revealed that the expression of Arg-1 protein was significantly higher in the ASCs group than that of PBS and ASCs$^{Si-HIF-1\alpha}$ groups (Figure 6D,E). These results indicate that the injection of ASCs can enhance the recruitment of macrophages to ischemic muscle and
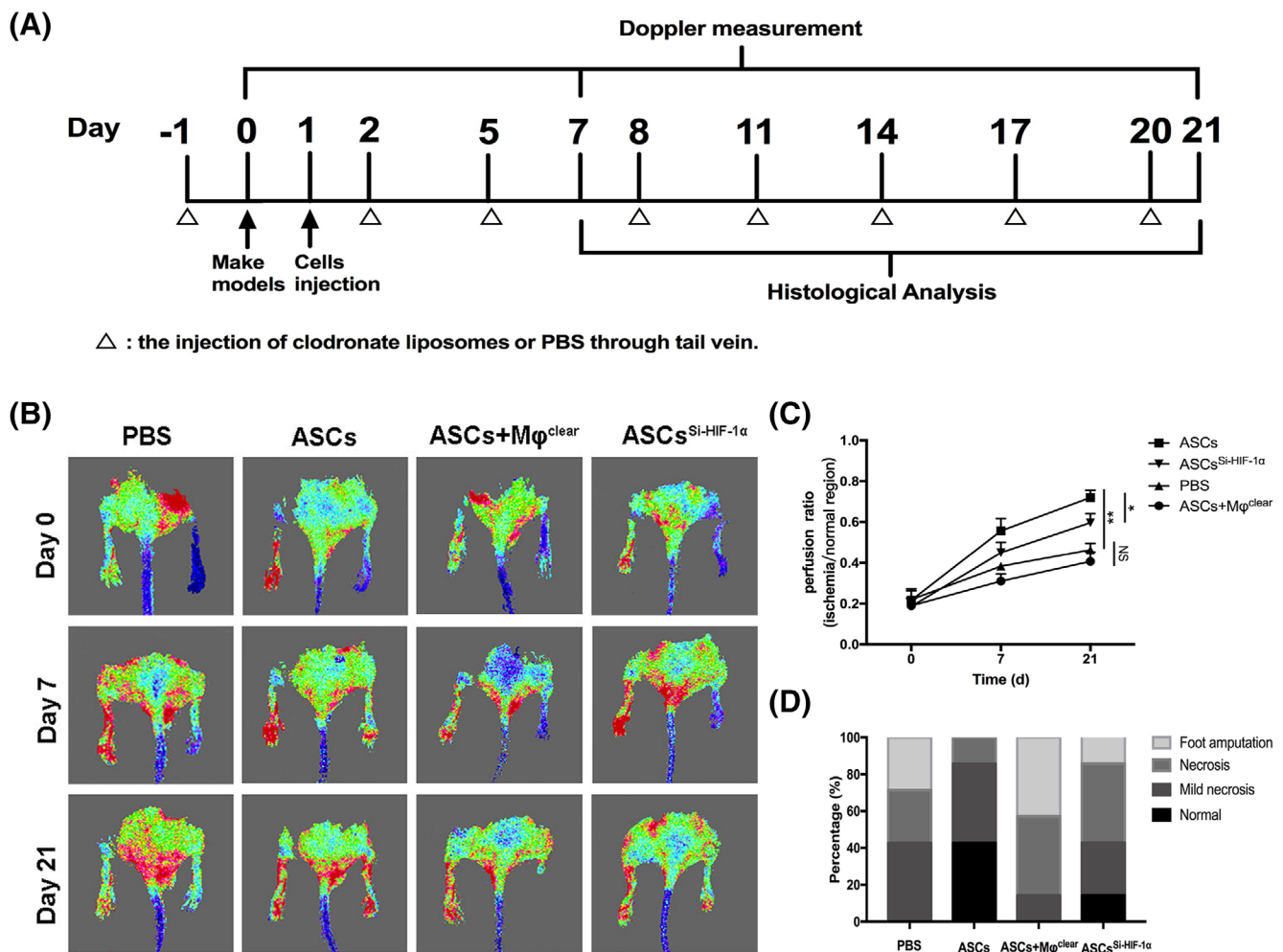
FIGURE 5 The depletion of tissue macrophages or transplant of HIF-1α-silenced ASCs reduced blood reperfusion and limb salvage. A, Schematic of the treatment of ischemic hind limbs and evaluation methods. B, Representative images of blood reperfusion on days 0, 7, and 21 after ligation. C, Quantitative analysis of blood flow measured by LDPI. The perfusion ratio means the average ratio of ischemic hind limb to contralateral hind limb). D, Ratio of limb salvage result on day 21. *P < .05; **P < .01; ***P < .001. ASCs + Mφ^{clear}, the mice group treated with ASCs and clodronate liposomes; ASCs, adipose-derived mesenchymal stem cells; ASCs$^{Si-HIF-1\alpha}$, the mice group treated with ASCs$^{Si-HIF-1\alpha}$; LDPI, laser Doppler perfusion imaging; NS, not significant; PBS, phosphate buffer saline
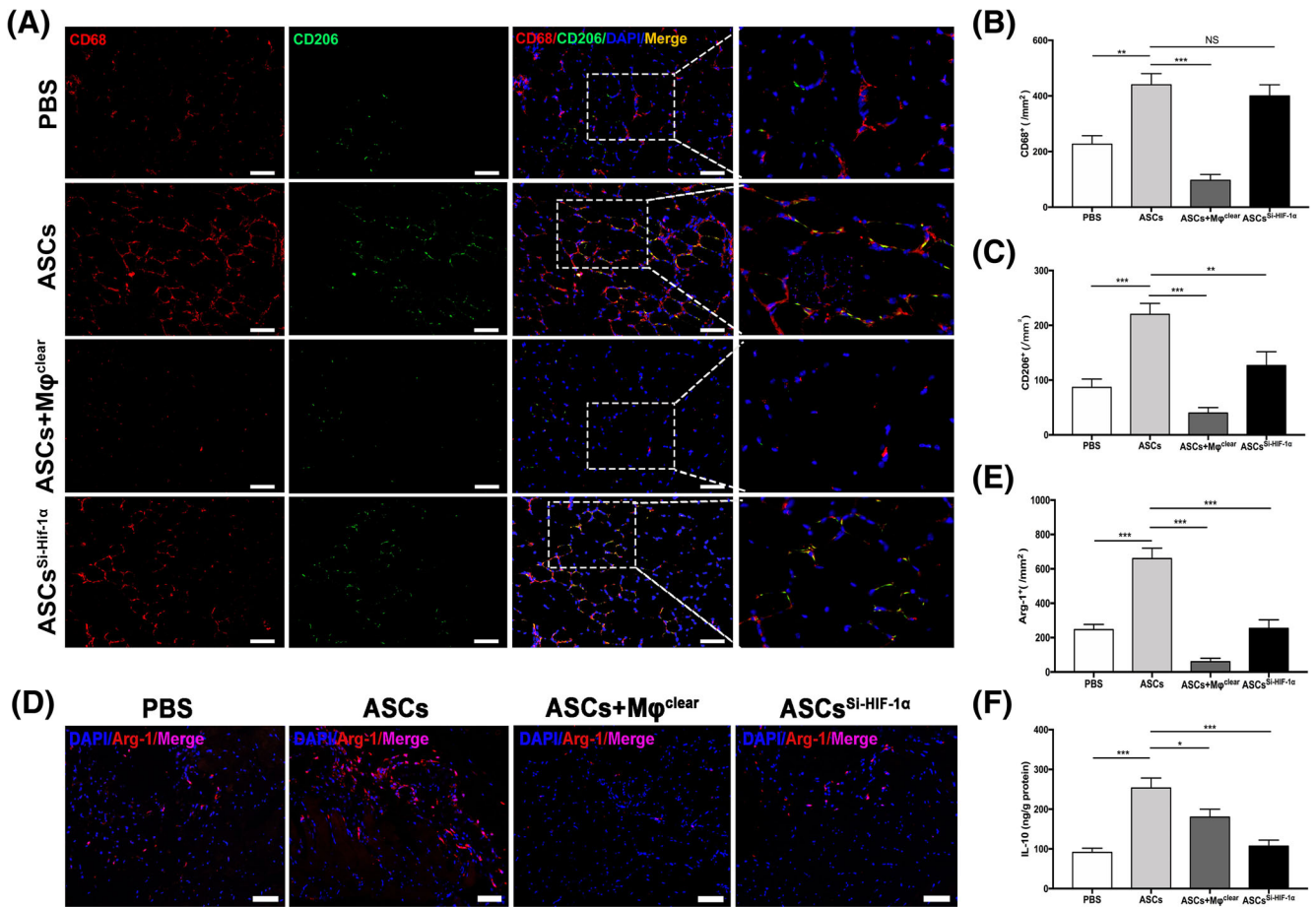
FIGURE 6 ASCs transplant increased the density of M2 macrophages induced higher amount of IL-10 in ischemic muscle. A, Representative images of CD68 (red) and CD206 (green) double-immunostaining in hind limb muscle. Nuclei were stained with DAPI (blue); B,C, Quantitative analysis of the density of CD68$^+$ cells (B) and CD206$^+$ cells (C) in ischemic muscle. D, Representative images of immunostaining for Arg-1 (red) in ischemic muscle. Nuclei were stained with DAPI (blue). E, Quantitative analysis of the density of Arg-1$^+$ cells. F, Quantitative analysis of the amounts of IL-10 in ischemic muscle. *$P < .05$; **$P < .01$; ***$P < .001$. Scale bar = 100 μm. Arg-1, Arginase-1; ASCs $^{Si-HIF-1\alpha}$, the mice group treated with ASCs $^{Si-HIF-1\alpha}$; ASCs + Mφ^{clear}, the mice group treated with ASCs and clodronate liposomes; ASCs, adipose-derived mesenchymal stem cells; IL-10, DAPI, 4',6-diamidino-2-phenylindole; Interleukin-10; NS, not significant; PBS, phosphate buffer saline

increase the proportion of M2 macrophages via a HIF-1α-mediated approach.

We also investigated the amount of IL-10 in the gastrocnemius muscle on day 7. The level of IL-10 in the ASCs$^{Si-HIF-1\alpha}$ group was obviously lower than that in the ASCs group (Figure 6F), indicating that silencing HIF-1α in ASCs impairs the expression of IL-10 in ischemic muscle, which is consistent with the in vitro results (Figure 3D,E). To evaluate tissue necrosis and angiogenesis in ischemic limbs, gastrocnemius muscles were harvested from all groups on day 21 for histological evaluation. H&E staining showed that the muscles from the ASCs + Mφ^{clear} and PBS groups had amounts of necrotic fibers but those from the ASCs and ASCs$^{Si-HIF-1\alpha}$ groups were mainly filled with normal or regenerative muscle fibers (Figure 7A). Quantitative analysis showed that the percentage area of necrosis in the ASCs + Mφ^{clear} and PBS groups was higher than that in the ASCs and ASC$^{Si-HIF-1\alpha}$ groups (Figure 7B). Moreover, immunohistochemical staining demonstrated that the capillary density in the ASCs group was significantly higher than that of the other groups, whereas silencing HIF-1α in

ASCs inhibit the effect (Figure 7C,D), which was consistent with the LDPI results of day 21 (Figure 5C). These results demonstrate that ASCs can enhance ischemic muscle repair by inducing M2 macrophage polarization, with HIF-1α and IL-10 playing critical roles.

4 | DISCUSSION

In recent years, the combination of regenerative and immunomodulatory properties of MSCs has triggered exploration of their therapeutic use. Significant advances have been made in the treatment of various diseases using MSCs and a breakthrough has been achieved with the marketing authorization of allogeneic stem cell therapy.[33] Ongoing experiments have attributed the therapeutic effect of MSCs to a specific component, but there is a long way to go in elucidating the mechanisms of MSCs. In the current study, we investigated the therapeutic mechanism and immunomodulatory properties of ASCs in ischemic muscle remodeling. Our data demonstrated that: (a) ASCs enhance
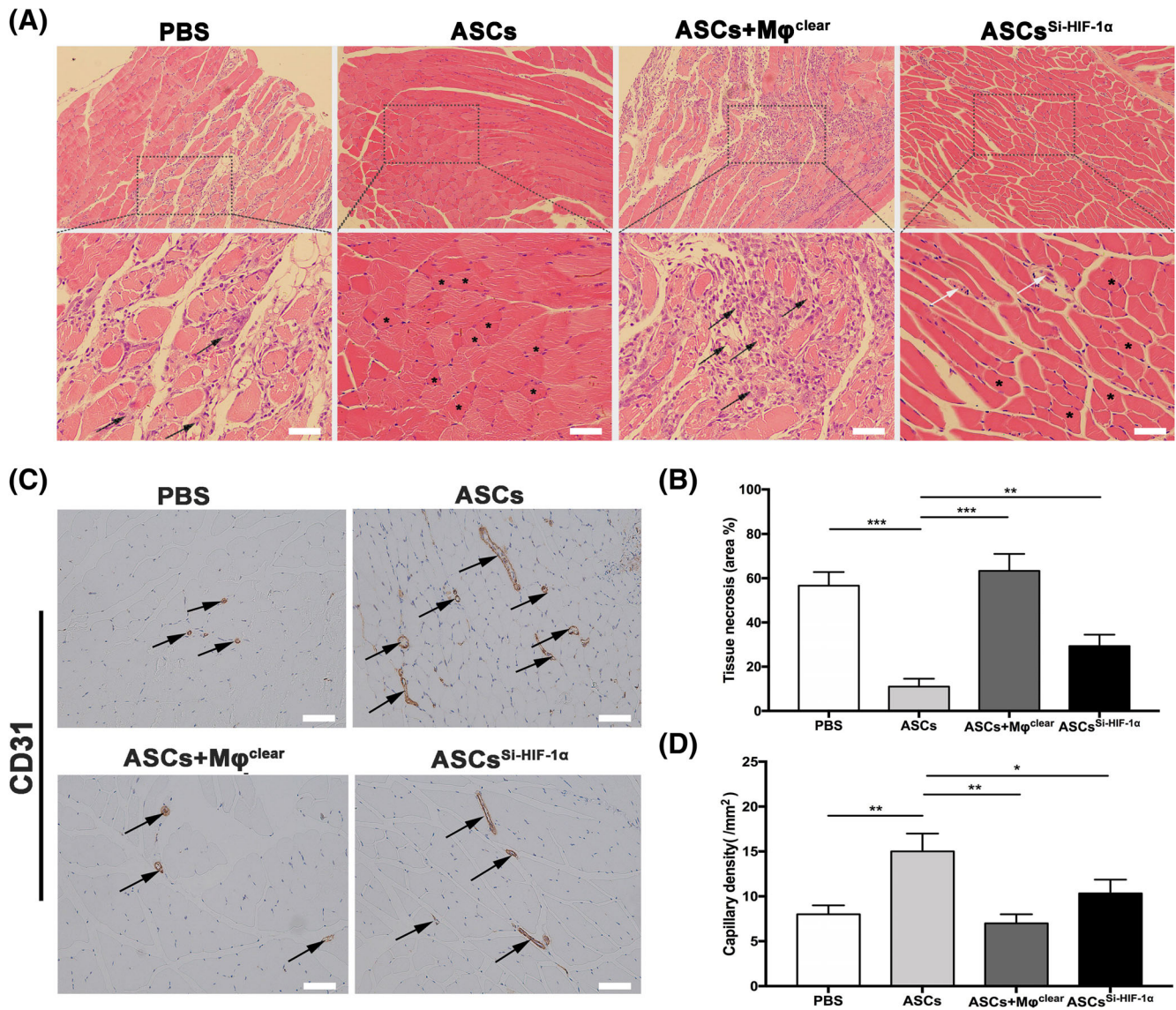
FIGURE 7 Histological analysis of necrosis and angiogenesis in ischemic hind limbs. A, Representative images of H&E staining to detect myofibers state in gastrocnemius muscles. Black arrows indicate necrotic myofibers with pale cytoplasm; White arrows indicate regenerative muscle fibers with one or more centrally located nuclei. Asterisks indicate normal myofibers with peripheral nuclei. B, Representative images of immunostaining of CD31 in gastrocnemius muscles. C, Quantitative analysis result of the percentage of necrotic tissue. Arrows indicate blood vessels. D, Quantitative analysis of capillary density. At least three independent experiments were performed with each experiment. *$P < .05$; **$P < .01$; ***$P < .001$. Scale bar = 100 μm. ASCs + Mφ^{clear}, the mice group treated with ASCs and clodronate liposomes; ASCs, adipose-derived mesenchymal stem cells; ASCs$^{Si-HIF-1α}$, the mice group treated with ASCs$^{Si-HIF-1α}$. PBS, phosphate buffer saline

the migration of RAW264.7 macrophages in hypoxia; (b) IL-10 expression in ASCs is upregulated in hypoxia and it is mediated by HIF-1α; (c) ASCs-derived IL-10 induces RAW264.7 macrophages to M2 phenotype via STAT3/Arg-1 pathway in hypoxia; (d) the induction of M2 macrophages by ASCs promotes ischemic muscle repair; and finally (e) HIF-1α/IL-10 pathway is responsible for the induction of M2 macrophage by ASCs in ischemic muscle.

Previous studies have shown that the interaction between MSCs and macrophages is crucial for effective immunomodulation and tissue regeneration.[34,35] To verify the importance of macrophages in ischemic muscle repair induced by ASCs, tissue macrophages were depleted using clodronate liposomes in mice. Compared with ASCs

group, ASCs + Mφ^{clear} group exhibited poorer limb prognosis, lower density of vessels, and more necrotic muscle fibers. Unexpectedly, the limb perfusion ratio and vessels density in ASCs + Mφ^{clear} group were lower than those of PBS group, whereas no significant difference was observed (Figure 7B,D). These results confirmed the crucial role of macrophages in ASCs-mediated tissue repair. Tissue macrophages derive from embryonic progenitors and blood monocyte infiltration, with homeostasis maintained through local proliferation and monocyte recruitment.[36] Our work found that the migration capacity of macrophages was enhanced by ASCs under hypoxic conditions, which was verified by the increased infiltration of macrophages in ischemic muscle after ASCs injection. In vitro result exhibited the efficiency of

ASCs for the induction of M2 macrophages in hypoxia and a higher proportion of M2 macrophages was also observed in ASCs-transplanted group compared with PBS group. Collectively, these results indicate that ASCs may have an immunoregulatory effect on ischemic muscle through enhancing the migration of macrophages and inducing the recruited macrophages toward M2 phenotype.

Upon the ligation of the femoral artery, the ischemic limb experiences a dramatic decrease in oxygen levels.[24,37] ASCs live in an environment of hypoxia and starvation after injected into ischemic muscle. Recent studies showed that the differentiation of MSCs was weakened and the paracrine function of MSCs was enhanced under hypoxic conditions, which contributed greatly to tissue repair.[26,38,39] For example, hypoxia-induced ASCs can protect salivary glands from irradiation-induced salivary hypofunction via enhanced secretion of fibroblast growth factor 10 (FGF-10).[26] One study focused on the contribution of paracrine effect vs direct differentiation of transplanted ASCs on cardiac repair, showing that the therapeutic effect was mainly attributed to paracrine-mediated cardioprotection rather than direct differentiation of ASCs.[39] Our study revealed that adipogenesis and osteogenesis differentiation of ASCs in hypoxia decreased significantly, whereas the paracrine function was enhanced with the increased secretion of multiple growth factors and anti-inflammatory cytokines. In vivo results showed that the transplant of HIF-1α-silenced ASCs reduced the level of IL-10 in muscle and decreased the therapeutic effect. These results indicate that the paracrine effect, other than the direct differentiation, may be the main therapeutic mechanism of ASCs on ischemic muscle repair.

Hypoxia-inducible factors (HIFs) are heterodimeric transcription factors that play a crucial role in cellular responses to hypoxia.[40] HIF-1α is an oxygen-labile alpha subunit of HIFs, which can become relatively stable in hypoxia and activate respective target genes involved in angiogenesis, erythropoiesis, and glycolysis.[41] Previous studies revealed that IL-10 could exert immunomodulatory and regenerative effect through the induction of macrophages polarization.[42] In our work, ASCs were cultured in hypoxia to mimic in vivo conditions and it turned out to have an increased expression of IL-10 in ASCs. Besides, the experiments of SiRNA transfection exhibited that the increased expression of IL-10 was mediated by HIF-1α under hypoxic conditions, which was in line with the results of previous study.[43] In vivo results showed that the IL-10 level in gastrocnemius muscle of ASCs group was remarkably higher than that of ASCs^Si-HIF-1α group. These results demonstrated the predominant role of HIF-1α for IL-10 expression in ASCs after transplanted into ischemic muscle.

Studies have shown that IL-10 can induce M2 macrophages polarization through multiple pathways.[44] We further investigated the mechanism of ASCs-derived IL-10 in inducing M2 macrophages polarization under hypoxic conditions. P-STAT3, identified as an initiator of macrophage activation, increased significantly after incubation in CM-ASCs under hypoxic conditions in our study. A previous study had proved that the IL-10/STAT3 axis is essential for the induction of M2 macrophages after myocardial infarction.[45] Another study demonstrated that the IL-10/STAT3 axis plays a crucial role in generating alternatively activated macrophages in a tumor microenvironment.[46] In our work, we definitively verified the dominant role of ASCs-derived IL-10 in the activation of STAT3 within macrophages. In addition, the expression of anti-inflammatory mediator Arg-1 increased significantly after macrophages were cultivated with CM-ASCs in hypoxia, whereas using anti-IL-10 or S3I-201 inhibited the effect. In vivo data showed that the expression of Arg-1 among groups was consistent with the density of M2 macrophages and the levels of IL-10 in ischemic muscle. These results imply that the IL-10/STAT3/Arg-1 pathway regulates the induction of M2 macrophages in hypoxia and plays the critical role in the immunoregulation of ASCs on ischemic muscle repair.

M2 macrophages, as the anti-inflammatory phenotype, could contribute to muscle repair through resolving inflammation, promoting angiogenesis, stimulating myogenesis, and fiber growth.[47,48] Based on activating stimulus, M2 macrophages can be further divided into four alternately activated subtypes: M2a (induced by exposure to IL-4 or IL-13); M2b (activated by immune complexes in the presence of a Toll-like receptor ligand); M2c (stimulated with IL-10, glucocorticoids, or TGF-β); M2d (elicited by Toll-like receptors [TLR] agonists through the adenosine receptor).[21,49] The macrophages in mice treated with ASCs expressing a high level of Arg-1, similar to M2c subset, which is characterized by high expression of Arg-1 and IL-10.[50] Moreover, our results showed that M2-like macrophages were induced by ASCs through the activation of IL-10/STAT3 pathway, which is consistent to previous reports of M2c polarization.[51,52] Therefore, the M2 macrophages in mice treated with ASCs resemble the M2c subtype, indicating the vital role of M2c macrophages in ASCs-mediated ischemic muscle repair.

However, there are some limitations in our work. First, only RAW264.7 cells were used for in vitro experiments. Although they were proved to be effective in evaluating the functions of macrophages as previously reported,[53,54] they are different from primary macrophages in some respects, such as rapid proliferation, continuous passage, and so on. Second, our work only focused on the mechanism of ASCs on macrophages polarization. Further study on the underlying mechanism of ASCs in recruiting macrophages to ischemic muscle is needed. Third, the crosstalk between ASCs and macrophages is not explored in our work, which is vital in ASCs-mediated ischemic tissue repair. Future research should be performed to examine the effect of macrophages on the properties (viability, proliferation, migration, and differentiation) of ASCs in hypoxia.

In this study, we provide data showing the immunomodulatory effect of allogeneic ASCs on ischemic muscle repair under hypoxic conditions. These findings not only confirmed the critical role of M2 macrophages in ASCs-induced tissue repair, but also elucidated the mechanism, which enhanced the understanding of ASCs-mediated tissue remodeling and contributed to the improvement of ASCs-based therapeutics. In addition, our work suggests the translational potential of topical IL-10 in ischemic muscle, providing an alternative to cell-based approaches.

5 | CONCLUSION

In conclusion, we have demonstrated that allogeneic ASCs could contribute to ischemic muscle repair by enhancing the recruitment of

macrophages and inducing macrophages toward M2 phenotype, with HIF-1α/IL-10 pathway playing the crucial role.

CONFLICT OF INTEREST

The authors declared no potential conflicts of interest.

AUTHOR CONTRIBUTIONS

J.L.: conducting experiments, data analysis and interpretation, manuscript writing; P.Q.: conducting experiments, data analysis and interpretation; X.L.: conception and design, final approval of manuscript; Z.P.: conception and design, manuscript revision, final approval of manuscript; K.Y.: conception and design; J.Q., B.L.: conducting experiments; X.Y., Xiaoyu Wu: collection and analysis of data; Xin Wang: manuscript writing; W.Z.: manuscript revision.

DATA AVAILABILITY STATEMENT

The data that support the findings of this study are available on request from the corresponding author.

ORCID

Xinwu Lu (iD) https://orcid.org/0000-0001-6503-5210

REFERENCES

1. Fowkes FG, Rudan D, Rudan I, et al. Comparison of global estimates of prevalence and risk factors for peripheral artery disease in 2000 and 2010: a systematic review and analysis. *Lancet*. 2013;382: 1329-1340.
2. Farber A, Eberhardt RT. The current state of critical limb ischemia: a systematic review. *JAMA Surg*. 2016;151:1070-1077.
3. Norgren L, Hiatt WR, Dormandy JA, et al. Inter-society consensus for the management of peripheral arterial disease (TASC II). *J Vasc Surg*. 2007;45(suppl S):S5-S67.
4. Cooke JP, Losordo DW. Modulating the vascular response to limb ischemia: angiogenic and cell therapies. *Circ Res*. 2015;116:1561-1578.
5. Nakagami H, Morishita R, Maeda K, Kikuchi Y, Ogihara T, Kaneda Y. Adipose tissue-derived stromal cells as a novel option for regenerative cell therapy. *J Atheroscler Thromb*. 2006;13:77-81.
6. Tapp H, Hanley EN Jr, Patt JC, Gruber HE. Adipose-derived stem cells: characterization and current application in orthopaedic tissue repair. *Exp Biol Med*. 2009;234:1-9.
7. Gentile P, Scioli MG, Bielli A, Orlandi A, Cervelli V. Concise review: the use of adipose-derived stromal vascular fraction cells and platelet rich plasma in regenerative plastic surgery. *Stem Cells*. 2017;35: 117-134.
8. Al-Daccak R, Charron D. Allogenic benefit in stem cell therapy: cardiac repair and regeneration. *Tissue Antigens*. 2015;86:155-162.
9. Sanz-Ruiz R, Fernandez-Aviles F. Autologous and allogeneic cardiac stem cell therapy for cardiovascular diseases. *Pharmacol Res*. 2018; 127:92-100.
10. Peng Z, Yang X, Qin J, et al. Glyoxalase-1 overexpression reverses defective proangiogenic function of diabetic adipose-derived stem cells in streptozotocin-induced diabetic mice model of critical limb ischemia. *Stem Cells Translational Medicine*. 2017;6:261-271.
11. Qin J, Yuan F, Peng Z, et al. Periostin enhances adipose-derived stem cell adhesion, migration, and therapeutic efficiency in Apo E deficient mice with hind limb ischemia. *Stem Cell Res Ther*. 2015;6:138.
12. Zheng Y, Qin J, Wang X, Peng Z, Hou P, Lu X. Dynamic imaging of allogeneic adipose-derived regenerative cells transplanted in ischemic hind limb of apolipoprotein E mouse model. *Int J Nanomedicine*. 2017; 12:61-71.
13. Park I-S, Chung P-S, Ahn JC. Enhanced angiogenic effect of adipose-derived stromal cell spheroid with low-level light therapy in hind limb ischemia mice [in English]. *Biomaterials*. 2014;35:9280-9289.
14. Bura A, Planat-Benard V, Bourin P, et al. Phase I trial: the use of autologous cultured adipose-derived stroma/stem cells to treat patients with non-revascularizable critical limb ischemia. *Cytotherapy*. 2014; 16:245-257.
15. Ulivi V, Tasso R, Cancedda R, Descalzi F. Mesenchymal stem cell paracrine activity is modulated by platelet lysate: induction of an inflammatory response and secretion of factors maintaining macrophages in a proinflammatory phenotype. *Stem Cells Dev*. 2014;23:1858-1869.
16. Ratajczak MZ, Kucia M, Jadczyk T, et al. Pivotal role of paracrine effects in stem cell therapies in regenerative medicine: can we translate stem cell-secreted paracrine factors and microvesicles into better therapeutic strategies? *Leukemia*. 2012;26:1166-1173.
17. Roh JD, Sawh-Martinez R, Brennan MP, et al. Tissue-engineered vascular grafts transform into mature blood vessels via an inflammation-mediated process of vascular remodeling. *Proc Natl Acad Sci USA*. 2010;107:4669-4674.
18. Landskron G, De la Fuente M, Thuwajit P, et al. Chronic inflammation and cytokines in the tumor microenvironment. *J Immunol Res*. 2014; 2014:149185.
19. Bajpai G, Bredemeyer A, Li W, et al. Tissue resident CCR2- and CCR2 + cardiac macrophages differentially orchestrate monocyte recruitment and fate specification following myocardial injury. *Circ Res*. 2019;124:263-278.
20. Dick SA, Macklin JA, Nejat S, et al. Self-renewing resident cardiac macrophages limit adverse remodeling following myocardial infarction. *Nat Immunol*. 2019;20:29-39.
21. Shapouri-Moghaddam A, Mohammadian S, Vazini H, et al. Macrophage plasticity, polarization, and function in health and disease. *J Cell Physiol*. 2018;233:6425-6440.
22. Parks SK, Cormerais Y, Pouyssegur J. Hypoxia and cellular metabolism in tumour pathophysiology. *J Physiol*. 2017;595:2439-2450.
23. Murdoch C, Muthana M, Lewis CE. Hypoxia regulates macrophage functions in inflammation. *J Immunol*. 2005;175:6257-6263.
24. Huang Y, Chen B, Zhang J. Oxygen tension variation in ischemic gastrocnemius muscle, marrow, and different hypoxic conditions in vitro. *Med Sci Monit*. 2014;20:2171-2176.
25. Berniakovich I, Giorgio M. Low oxygen tension maintains multipotency, whereas normoxia increases differentiation of mouse bone marrow stromal cells. *Int J Mol Sci*. 2013;14:2119-2134.
26. Shin HS, Lee S, Kim YM, Lim JY. Hypoxia-activated adipose mesenchymal stem cells prevents irradiation-induced salivary hypofunction by enhanced paracrine effect through fibroblast growth factor 10. *Stem Cells*. 2018;36:1020-1032.
27. Qiu X, Liu S, Zhang H, et al. Mesenchymal stem cells and extracellular matrix scaffold promote muscle regeneration by synergistically regulating macrophage polarization toward the M2 phenotype. *Stem Cell Res Ther*. 2018;9:88.
28. Mahdavian Delavary B, van der Veer WM, van Egmond M, et al. Macrophages in skin injury and repair. *Immunobiology*. 2011;216: 753-762.
29. Shin TH, Kim HS, Kang TW, et al. Human umbilical cord blood-stem cells direct macrophage polarization and block inflammasome activation to alleviate rheumatoid arthritis. *Cell Death Dis*. 2016;7:e2524.

30. Thomas D, Thirumaran A, Mallard B, et al. Variability in endogenous perfusion recovery of immunocompromised mouse models of limb ischemia. *Tissue Eng Part C Methods*. 2016;22:370-381.

31. Corcoran SE, O'Neill LA. HIF1alpha and metabolic reprogramming in inflammation. *J Clin Invest*. 2016;126:3699-3707.

32. Vasquez-Dunddel D, Pan F, Zeng Q, et al. STAT3 regulates arginase-I in myeloid-derived suppressor cells from cancer patients. *J Clin Invest*. 2013;123:1580-1589.

33. Hoogduijn MJ, Lombardo E. Mesenchymal stromal cells anno 2019: dawn of the therapeutic era? Concise review. *STEM CELLS TRANSLATIONAL MEDICINE*. 2019;8:1126-1134.

34. Nemeth K, Leelahavanichkul A, Yuen PS, et al. Bone marrow stromal cells attenuate sepsis via prostaglandin E(2)-dependent reprogramming of host macrophages to increase their interleukin-10 production. *Nat Med*. 2009;15:42-49.

35. Kim J, Hematti P. Mesenchymal stem cell-educated macrophages: a novel type of alternatively activated macrophages. *Exp Hematol*. 2009;37:1445-1453.

36. Sieweke MH, Allen JE. Beyond stem cells: self-renewal of differentiated macrophages. *Science*. 2013;342:1242974.

37. Simon F, Oberhuber A, Floros N, et al. Acute limb ischemia-much more than just a lack of oxygen. *Int J Mol Sci*. 2018;19:374.

38. Holzwarth C, Vaegler M, Gieseke F, et al. Low physiologic oxygen tensions reduce proliferation and differentiation of human multipotent mesenchymal stromal cells. *BMC Cell Biol*. 2010;11:11.

39. Yang D, Wang W, Li L, et al. The relative contribution of paracine effect versus direct differentiation on adipose-derived stem cell transplantation mediated cardiac repair. *PLoS One*. 2013;8:e59020.

40. Majmundar AJ, Wong WJ, Simon MC. Hypoxia-inducible factors and the response to hypoxic stress. *Mol Cell*. 2010;40:294-309.

41. Dengler VL, Galbraith M, Espinosa JM. Transcriptional regulation by hypoxia inducible factors. *Crit Rev Biochem Mol Biol*. 2014;49:1-15.

42. Jung M, Ma Y, Iyer RP, et al. IL-10 improves cardiac remodeling after myocardial infarction by stimulating M2 macrophage polarization and fibroblast activation. *Basic Res Cardiol*. 2017;112:33.

43. Xu L, Wang X, Wang J, et al. Hypoxia-induced secretion of IL-10 from adipose-derived mesenchymal stem cell promotes growth and cancer stem cell properties of Burkitt lymphoma. *Tumour Biol*. 2016;37:7835-7842.

44. Ip WKE, Hoshi N, Shouval DS, Snapper S, Medzhitov R. Anti-inflammatory effect of IL-10 mediated by metabolic reprogramming of macrophages. *Science*. 2017;356:513-519.

45. Shirakawa K, Endo J, Kataoka M, et al. IL (interleukin)-10-STAT3-galectin-3 axis is essential for osteopontin-producing reparative macrophage polarization after myocardial infarction. *Circulation*. 2018;138:2021-2035.

46. Lippitz BE. Cytokine patterns in patients with cancer: a systematic review. *Lancet Oncol*. 2013;14:e218-e228.

47. Ganta VC, Choi MH, Kutateladze A, Fox TE, Farber CR, Annex BH. A microRNA93-interferon regulatory factor-9-immunoresponsive gene-1-itaconic acid pathway modulates M2-like macrophage polarization to revascularize ischemic muscle. *Circulation*. 2017;135:2403-2425.

48. Arnold L, Henry A, Poron F, et al. Inflammatory monocytes recruited after skeletal muscle injury switch into antiinflammatory macrophages to support myogenesis. *J Exp Med*. 2007;204:1057-1069.

49. Abdelaziz MH, Abdelwahab SF, Wan J, et al. Alternatively activated macrophages: a double-edged sword in allergic asthma. *J Transl Med*. 2020;18:58.

50. Rőszer T. Understanding the mysterious M2 macrophage through activation markers and effector mechanisms. *Mediators Inflamm*. 2015;2015:816460.

51. Koscsó B, Csóka B, Kókai E, et al. Adenosine augments IL-10-induced STAT3 signaling in M2c macrophages. *J Leukoc Biol*. 2013;94:1309-1315.

52. Hayashi H, Naoi S, Togawa T, et al. Assessment of ATP8B1 deficiency in pediatric patients with cholestasis using peripheral blood monocyte-derived macrophages. *EBioMedicine*. 2018;27:187-199.

53. Xie Y, Wen H, Yan K, et al. Toxoplasma gondii GRA15 effector-induced M1 cells ameliorate liver fibrosis in mice infected with Schistosomiasis japonica. *Cell Mol Immunol*. 2018;15:120-134.

54. Ganta VC, Choi M, Farber CR, Annex BH. Antiangiogenic VEGF165b regulates macrophage polarization via S100A8/S100A9 in peripheral artery disease. *Circulation*. 2019;139:226-242.

SUPPORTING INFORMATION

Additional supporting information may be found online in the Supporting Information section at the end of this article.